RSC Advances

This is an *Accepted Manuscript*, which has been through the Royal Society of Chemistry peer review process and has been accepted for publication.

Accepted Manuscripts are published online shortly after acceptance, before technical editing, formatting and proof reading. Using this free service, authors can make their results available to the community, in citable form, before we publish the edited article. This *Accepted Manuscript* will be replaced by the edited, formatted and paginated article as soon as this is available.

You can find more information about *Accepted Manuscripts* in the **Information for Authors**.

ROYAL SOCIETY
OF **CHEMISTRY**

www.rsc.org/advances

Energy-efficient degradation of Rhodamine B in a LED illuminated Photocatalytic Fuel Cell with anodic Ag/AgCl/GO and cathodic $ZnIn_2S_4$ catalysts

Yuanyuan Liu [a], Lifen Liu [a, b, *], Fenglin Yang[a]

[a] Key Laboratory of Industrial Ecology and Environmental Engineering (MOE), School of Environmental Science and Technology, Dalian University of Technology, Dalian 116024, China

[b] School of Food and Environment, Dalian University of Technology, Panjin, China

Abstract

Photocatalytic fuel cell (PFC) is a newly developed technology that degrades pollutants and simultaneously generates electricity. Stainless steel electrodes loaded respectively with anodic Ag/AgCl/GO and cathodic $ZnIn_2S_4$, formed one-chambered PFC, in which rhodamine B (RhB) was degraded under visible light (2W LED). After 1h irradiation, 87.4% of RhB was degraded and $0.52mA/cm^2$ current density was generated when the external resistance was 1Ω. Increasing this resistance lowered current density and decreased degradation. The current and cell voltage is affected by the degradation efficiency over electrodes, that the photocatalytic electrode with higher degradation activity functioned as anode, because of its relatively richer supply of electrons than the other. The Ag/AgCl/GO can function as cathode in a two-chambered PFC reactor with Fe as anode, which also had high degradation efficiency and higher electricity generation performance. Characteristics of the photoelectrodes were investigated using scanning or transparent electronic microscopy (SEM, TEM), continuous cyclic voltammograms (CV) and Electrochemical Impedance Spectroscopy (EIS). Electron Spin Resonance (ESR) was used to detect the reactive oxygen species (ROS). The effect of pH and RhB concentration on the degradation performance of this PFC was investigated. The PFCs can work in a broad range of pH.

Keywords: Photocatalytic Fuel Cell; Ag/AgCl/GO-based photoanode; Rhodamine B

1. Introduction

The deterioration situations of environmental pollution and energy crisis have become this generation's primary concerns, and will probably last to the next generation, due to the

discharge of pollutants and the excessive consumption of energy, which negatively impacts environments.[1] To overcome these problems in wastewater treatment, new energy-efficient wastewater treatment technologies need to be developed.

One attractive technology recently emerged is the photocatalytic fuel cell (PFC) which treats waste water using light and produces electricity.[2-5] Generally, a PFC consists of an anode loaded with semiconductor photocatalyst, a cathode carrying a different photo/electro-catalyst and an aqueous electrolyte. Titanium dioxide based catalysts had been used as photoanode,[2, 4, 6] not only because of its superior stability, low cost and high oxidation power (2.9-3.1eV),[7] but also because it is an n-type semiconductor. But, TiO_2-based photoanode can only be driven by UV light. To increase light response in visible range, TiO_2 modifications are required.

To enhance anode catalytic activity and PFC performance,[8] more effective alternative photocatalysts should be tested, for intensifying degradation, suitable matching of anodic catalysts with more positive VB potential for anodic oxidation reaction with cathodic catalysts with more negative CB potential for cathodic reduction should be studied.[5]

Currently, Ag/AgCl, a visible-light-driven plasmonic photocatalyst, displays excellent photocatalytic performance and has been recognized as one of the most promising alternatives to the traditional photocatalysts.[9-12] The energy gap of Ag/AgCl is 3.25eV which is comparable with TiO_2 (2.9-3.2eV).[13, 14] The distinct surface Plasmon resonance (SPR) absorptions over a wide range of visible-light region could be attributed to the existence of metallic Ag nanoparticles. Recently graphene-based composite photocatalysts have received increasing attention.[15-17] And, introducing Graphene oxide (GO) in the synthesis of Ag/AgCl as capping agent or catalyst promoter improved the catalytic performance, because of its abundant oxygen-containing functional groups such as hydroxyl, epoxide, carbonyl, carboxyl, etc. The hybrid Ag/AgCl/GO plasmonic photocatalyst has excellent activity toward organic contaminant under visible light. As the valence band (VB) of Ag/AgCl/GO is 3.19eV (vs TiO_2 3.1eV), it has a high oxidation power to degrade organic pollutants,[14] Ag/AgCl/GO is a suitable alternative for TiO_2 photoanode catalyst.

In PFC, the photoanode and cathode are connected through the external circuit. When ca-

thode is loaded with a photocatalyst, it can be activated to generate electron-hole pairs by illumination. The generated electrons on anode transmit to the photocathode via the external circuit, which either recombine with the holes in photocathode or are consumed by cathodic reactions, while the anode photo-generated holes migrate to the surface and degrade pollutants. The photo-generated electrons may participate in the cathodic reactions, forming H_2O or radicals by reducing oxygen, or forming H_2 by reducing protons. Hence, an appropriate photocatalyst of photocathode is important to the performance of PFC.

$ZnIn_2S_4$, with a conduction band (CB) at -0.91eV,[18] is considered suitable for photocathode. In previous studies,[19] $ZnIn_2S_4$ had remarkable hydrogen production rate. It is a very stable and highly active visible light photocatalyst. In addition, $ZnIn_2S_4$ film on the fluorine doped tin oxide glass prepared through chemical bath deposition (CBD) by Cheng et al. had good photo-electrochemical properties.[20]

Based on the theoretical suggestions that photoanode should have a positive potential of VB and photocathode should have a negative potential of CB, we constructed a PFC reactor with anodic Ag/AgCl/GO and cathodic $ZnIn_2S_4$ to degrade RhB in one chambered reactor. In this way, the organic "substrates" can be decomposed and the chemical energy in organic "substrates" can be converted into electricity simultaneously. To improve the performance of PFC, the photo-electrodes with higher catalytic activities were used. At the same time, to reduce the input power of the PFC, a visible LED light (2W) was used as the light source.

2. Experimental Section

2.1 Materials

Photoelectrode was prepared using Stainless steel mesh (SSM, 500 mesh, Shanghai Suita Filter Material Co., Ltd. China) and coated with photocatalyst. All other chemicals used were of analytical grade and used as received. Silicon sol solution was bought from Dalian Sinuo chemical materials science&technology co., LTD.

2.2 Preparation of photocatalysts Ag/AgCl/GO and $ZnIn_2S_4$

First, Graphene oxide (GO) solution was prepared using a modified Hummers' method.[21] Then, Ag/AgCl/GO photocatalyst was prepared using a two-step method which included de-

position-precipitation reaction and photo-reduction.[9, 11] In a typical and simple procedure, $Ag(NH_3)_2NO_3$ solution was used as the Ag source, prepared by dropping ammonia solution (6.9 mL, 25wt% NH_3) into the $AgNO_3$ solution (50mL, $0.074 mol \cdot L^{-1}$). GO aqueous solution (8.4 mL, with concentration of $1 g \cdot L^{-1}$) was added drop-wise to the $Ag(NH_3)_2NO_3$ solution and stirred for 30 min. Subsequently, a 4.5mL concentrated hydrochloric acid (HCl) was drop-wise introduced into the above solution. After the addition of HCl, the intensive stirring was continued and maintained for 24 h to form homogeneous suspension. Then, the above solution was mixed with 50 mL ethanol and irradiated with a 100 W Tungsten-Halogen for 30min. Then the purple-black product (Ag/AgCl/GO) was collected by centrifugation, washed with deionized water and dried in air.

$ZnIn_2S_4$ was synthesized via a hydrothermal method according to our previous research.[22]

2.3 Preparation of photoanode and photocathode

The stainless steel mesh was used as the base electrode to support catalyst. Prior to use, the stainless steel mesh was cut into 2cm×5cm, polished with sandpaper and cleaned ultra-sonically in sequence in ethanol, hydrochloric acid (3%) and distilled water respectively (each for 5 min), then dried naturally. The prepared Ag/AgCl/GO photocatalyst was dispersed into silicon sol solution in proportion of 1:1 (g/mL) to form uniform sol. Then the mixed sol was coated on the clean-and-dried stainless steel substrate with brush. After brush-coating, the stainless steel mesh was dried in air naturally. The process was repeated three times to prepare the Ag/AgCl/GO-based photoanode. After brush-coated, the weight of the stainless steel mesh increased about 0.1g. The $ZnIn_2S_4$-based photocathode was prepared in the same way except using $ZnIn_2S_4$ photocatalyst instead of Ag/AgCl/GO.

2.4 Apparatus of one-chambered reactor

The performance of the PFC system was studied in a single-chambered reactor with two photoelectrodes. A LED lamp (2W, brilliant white, φ18mm×25cm) was chosen as a visible light source and the illumination area was 20mm×50mm. The PFC oxidation reaction under visible light was performed by using the 2W LED light. In Fig. 1(a), a schematic diagram of the experimental apparatus and electrodes assembly for the PFC system is shown. The cell in a quartz tube (φ30mm×18cm) was equipped with an aeration device, Ag/AgCl/GO-based

photoanode and $ZnIn_2S_4$-based photocathode. The distance between anode and cathode was approximately 2.5 cm. The paired photo electrodes were dipped into aqueous solution of RhB in 0.1mol/L sodium sulfate. The volume of reaction solution was 50mL if not otherwise specified. The initial concentration of RhB was 10mg·L^{-1} and the initial pH was 7 unless otherwise specified. Prior to irradiation, the photoelectrodes were vertically fixed in the reactor and aerated/stirred for 30 min in the dark to establish the equilibrium of adsorption/desorption. When the system was running, the photoanode and photocathode was connected with 1Ωresistance and illuminated by a LED light of 2W separately as shown in Fig. 1(a). The value of the cell current and cell voltage was measured using a digital multimeter. All tests were repeated at least three times to ensure the reproducibility.
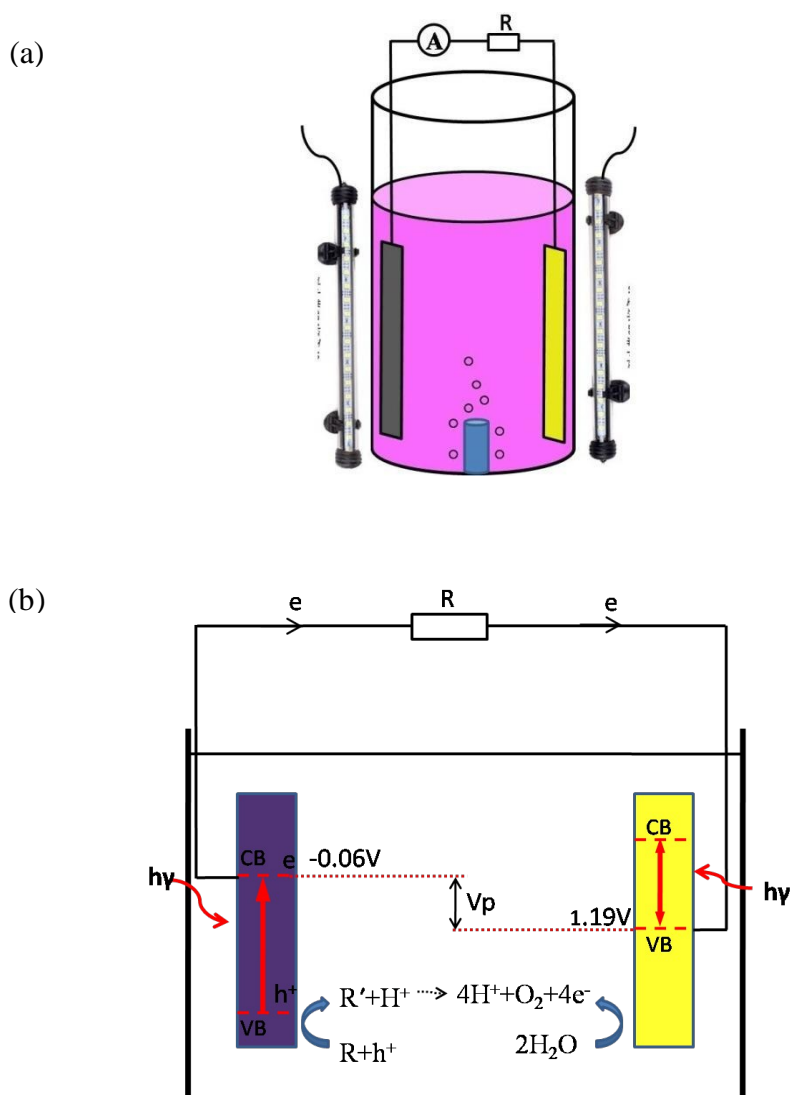
(a)

(b)

Figure 1. The schematic diagram of the photocatalytic fuel cell system

RSC Advances Accepted Manuscript

2.5 Apparatus of two-chambered reactor

The two-chambered PFC was made of quartz glass and each chamber was 100 mm × 50 mm ×200 mm. Cation exchange membrane (DF-120, Shandong Tian Wei membrane technology Co.,118 LTD. China) was sandwiched between the anode and cathode chamber(Fig.S4). In the PFC reactor with anodic Fe and cathodic Ag/AgCl/GO, the anode is perforated iron plate (0.1 cm (thickness) ×4 cm (width) ×20 cm (height)，aperture diameter 5 mm). The volume of anolyte was 100ml containing $0.06mol \cdot L^{-1}$ $NaHCO_3$, $0.05mol \cdot L^{-1}$ NaCl, and the initial pH was 5. Catholyte contained 10mg/L RhB and $0.1 \ mol \cdot L^{-1}$ NaCl. The initial pH was 7. Prior to irradiation, the photoelectrodes were vertically fixed in the reactor, after aeration and stirring for 30 min in the dark, the equilibrium of adsorption/desorption was established. Then for normal PFC operation, two LED lights were turned on and the external resistance was 500 Ω.

2.6 Characterization

The morphologies of the as-prepared Ag/AgCl/GO based photoanode and $ZnIn_2S_4$ based photocathode were observed using a scanning electron microscope (SEM) and transmission electron microscope (TEM). The electrochemical properties were characterized by continuous cyclic voltammograms (CV), Linear Sweep Voltammetry (LSV) and Electrochemical Impedance Spectroscopy (EIS) with electrochemical work station (Chenhua of Shanghai Co., Ltd., China). An electron spin resonance spectrometer (ESR, Bruker Elexsys A200, Germany) was used to characterize the reactive oxygen species (ROS) generated during the irradiation. DMPO (20mM) was used as a spin-trapping agent for the detection of •OH and $O_2 \bullet^-$.

RhB has commonly been used as a dye, especially for textile and industrial dyes. However, it is potentially toxic and carcinogenic.[23] Thus, RhB dye was often chosen as a representative organic pollutant to evaluate the PC/PEC performances of the as-fabricated nanocatalysts.[24, 25] The concentration of RhB was measured with an ultraviolet-visible spectrophotometer at 554nm. Potassium permanganate index (COD_{Mn}) was measured by national standard method.

6

3.   Results and Discussion

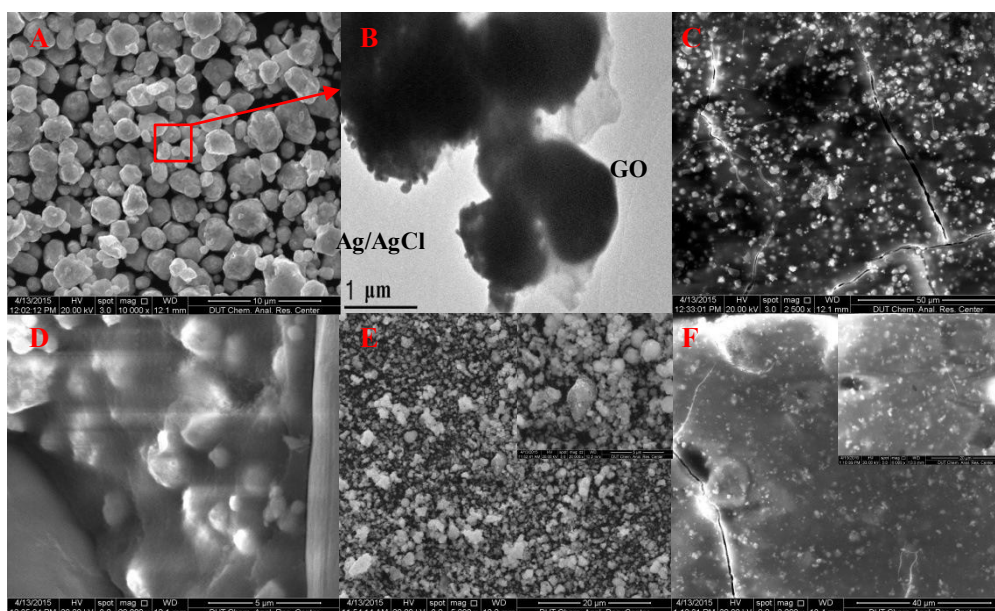### 3.1   Structure and morphology of photocatalysts and photoelectrodes

Figure 2. SEM image of Ag/AgCl/GO(A), Ag/AgCl/GO-coating-electrode(C~D), $ZnIn_2S_4$(E), $ZnIn_2S_4$-coating-electrode(F); TEM of Ag/AgCl/GO(B)

The morphology of the Ag/AgCl/GO hybrids was observed by SEM and TEM. As shown in Fig.2 (A), Ag/AgCl/GO has a near-spherical morphology with a size of 1~1.8μm. Ag/AgCl particle is distinctly wrapped with gauze like GO nanosheets (Fig.2 (B)). The SEM image of Ag/AgCl/GO-coated photoanode indicates a uniform morphology (Fig.2 (C, D)). It is identified that the brush-coated photoanode remains relatively stable and only has few cracking in the grid's intersections. The photocatalysts on the electrode distribute as fine particles due to particle aggregation. In the UV−visible diffuse reflectance spectra (Fig. S5), broad and strong absorptions in visible region was detected, which illustrated Ag/AgCl/GO had high intensity and wide absorbency ranged from UV to visible region due to the presence of GO and reduced Ag which increased absorbency in visible range from the SPR (Surface Plasmonic Resonance). In Fig.2 (E) and (F), $ZnIn_2S_4$ particles and $ZnIn_2S_4$-coated photocathode were shown. The size of $ZnIn_2S_4$ is smaller (about 0.8~1.2μm).

3.2 Properties of Ag/AgCl/GO-based photoanode and $ZnIn_2S_4$-based photocathode

The ORR activities of photoelectrodes were tested using CV in 0.5mol/L Na_2SO_4 electrolyte at a scan rate of 50mV/s. As shown in Fig. 3(a), Ag/AgCl/GO on the photoelectrode displays clearly redox peak corresponding to excellent redox activity, especially after oxygen purging. The photocatalyst-coated stainless steel wire mesh had better electrochemical activity than the blank stainless steel wire mesh, indicating the coated photocatalyst could greatly increase electrochemical activities. The peak at 0.155V, 0.68V and 0.2V (vs. SCE) confirmed significant ORR activity of the photoelectrode. But in nitrogen purged electrolyte, the reduction peak current was smaller and the oxidation peak was not obvious. So the presence of dissolved oxygen is advantageous to the redox activity. The oxygen reduction peaks (0.153V) can be more clearly observed by subtracting the capacitive current from the oxygen sparged curve (insert of Fig. 3(a)).

EIS is a highly effective method for studying the photoelectrochemical properties of surface-modified electrodes because the arc shape on the EIS Nyquist plot is largely dependent on the composition of the electrode.[26] As reported previously, the size of the arc diameter on the EIS Nyquist plots reflected the resistance of electron transfer and separation efficiency of photoinduced electron-hole pairs at the contact interface between the electrode and electrolyte solution.[27, 28] In this study, EIS was carried out to investigate the electron transfer resistance controlling the kinetics at electrode interface, which correspond to the diameter of arc at higher frequencies in the EIS plane,[29-31] as shown in Fig. 3(b). In EIS measurements performed in a 0.5 M Na_2SO_4 solution at a potential of 0.1 V, the half circle arc diameter of $ZnIn_2S_4$ electrode was smaller, because of its fair conductivity. Both $ZnIn_2S_4$ electrode and Ag/AgCl/GO electrode had a small arc diameter, meaning the good electron accepting and transporting properties of the photoelectrodes, which contribute to the effective charge separation, and subsequently the higher catalytic activity in degradation of pollutants.

Fig. 3(c) revealed the Linear sweep voltammetric curves of the Ag/AgCl/GO-based electrode under dark and visible light. The LSV curves were obtained in a 0.5M solution at 50mV/s. Clearly, the current intensity under illumination of visible light was larger than that in dark, indicating photoresponse and current production under visible light.
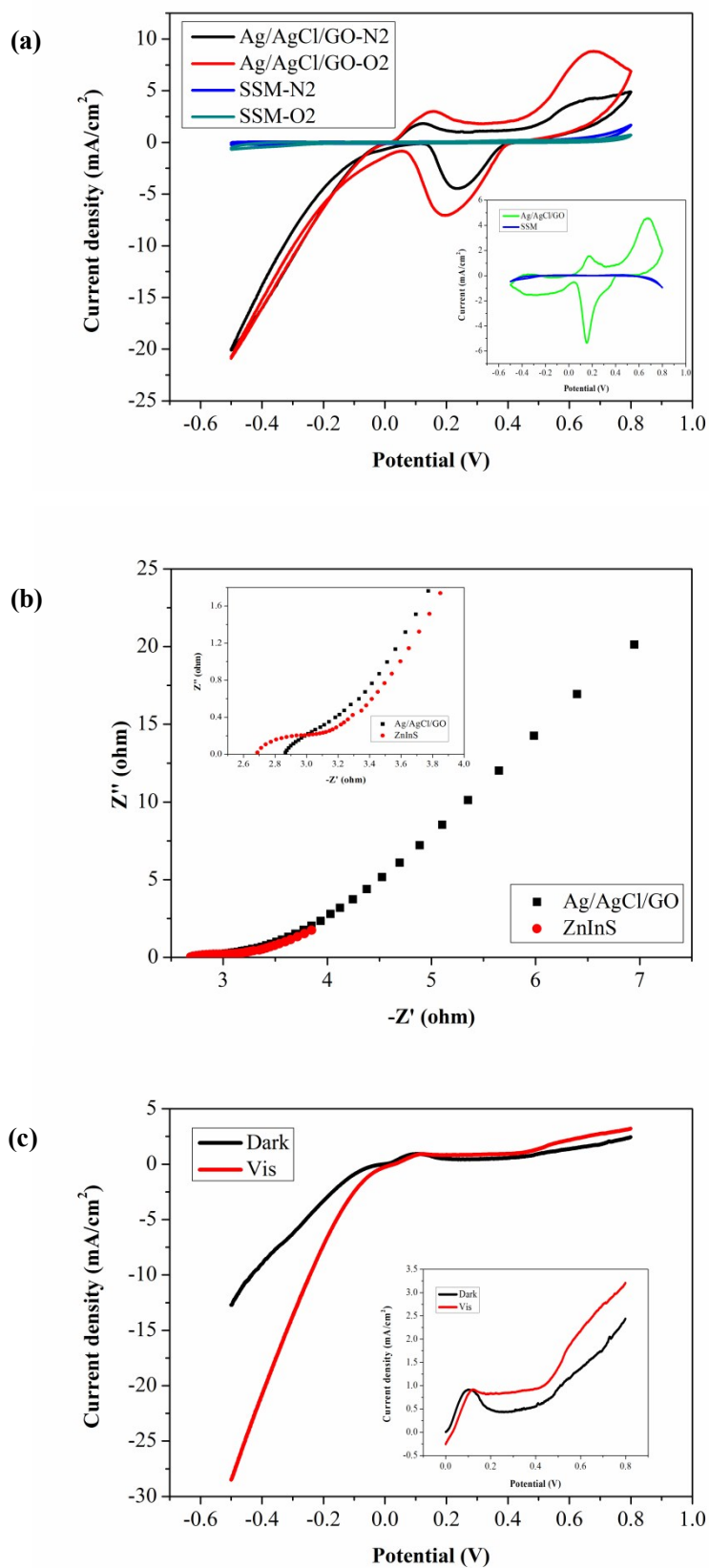
(a)

(b)

(c)

Figure 3. (a) Continuous cyclic voltammograms (CV) of Ag/AgCl/GO-coating-electrode; (b) EIS

changes of our Ag/AgCl/GO and ZnIn$_2$S$_4$ electrodes; (c) linear sweep voltammetric curves of

Ag/AgCl/GO-coating-electrode under visible light and dark condition. SSM: the stainless steel wire without photocatalyst; Ag/AgCl/GO: the stainless steel wire with Ag/AgCl/GO

### 3.3 Working principle of PFC systems and theperformance

3.3.1 Operating principle of the PFC

The PFC system works because of the mismatched Fermi levels between Ag/AgCl/GO (-0.06 VS.NHE for E_{CB}, +3.19 VS.NHE for E_{VB}) and $ZnIn_2S_4$(-0.91 VS.NHE for E_{CB}, +1.19 VS.NHE for E_{VB}) which provides an interior bias for the PFC (Fig. 1(b)). The high VB of Ag/AgCl/GO photoanode and low CB of $ZnIn_2S_4$ photocathode cause the potential difference between the electrodes. The higher degradation activity of Ag/AgCl/GO electrode defines its anodic function for supplying relatively richer electrons than $ZnIn_2S_4$ electrode. Upon irradiation, excited and generated electrons transport to the cathode through the external circuit, driven by the internal bias. The Ag/AgCl/GO could generate powerful holes to oxidize organics due to its relatively high valence band potential. The holes can degrade RhB directly. At the cathode, the electrons were accepted and consumed by holes and oxygen reduction. Depending on the catalyst and pH, H_2O, H_2O_2 or superoxide radical may be formed via ORR. This ORR related degradation kinetics and mechanism need to be further examined, because of possible interaction and involvement in oxidation reaction of pollutants with ROS on the catalyst surface.

3.3.2 Degradation efficiency, current density of the constructed PFC and its stability

Degradation efficiency and electricity generation are two important parameters to characterize the performance of PFC. RhB (50mL,10mg/L) was used to evaluate the performance of PFC with Ag/AgCl/GO-based photoanode and $ZnIn_2S_4$-based photocathode under visible light (2W LED). As shown in Fig. 4, 87.4% RhB was removed in 60 minutes with an external resistance of 1Ω. And the COD_{Mn} was reduced by 58.9%. It proved that RhB could be thoroughly degraded with enough time. If the external resistance is large enough to form a relatively large output voltage, the degradation of RhB would be adversely influenced. RhB degradation depends mainly on the oxidation by holes and hydroxyl radical. Large external resistance would reduce the amount of electrons transferred from anode, which would decrease the separation efficiency of h^+ and e^- in the anode. Only 67.8% of RhB were degraded

in the open circuit PFC. Accordingly, the external resistance of 1Ωwas used in the PFC, the electricity production performance was 0.52mA/cm^2 (averaged over the area of photoanode) in current density (Fig. 4(a)). The I-t curve had a slight fluctuation because of the influence of sampling and RhB concentration changes. The observed open circuit voltage under visible light was at about 0.35V. The cycling experiments suggested that the photocatalytic activity decreased slightly after five consecutive cycling tests (Fig. 4(b,c)).
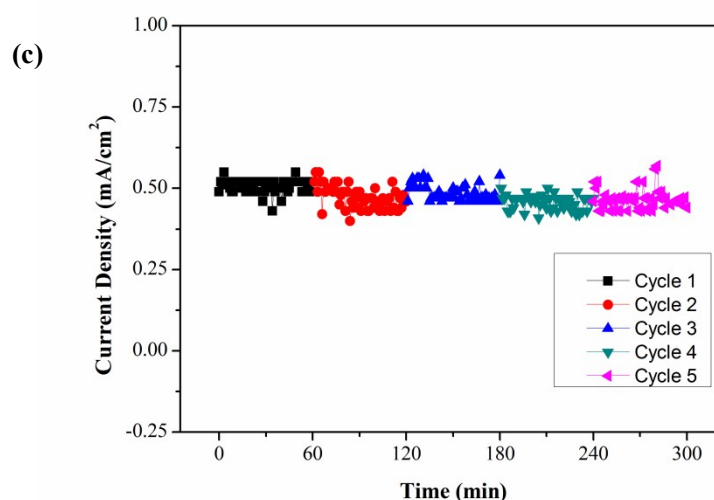

(a)

(b)
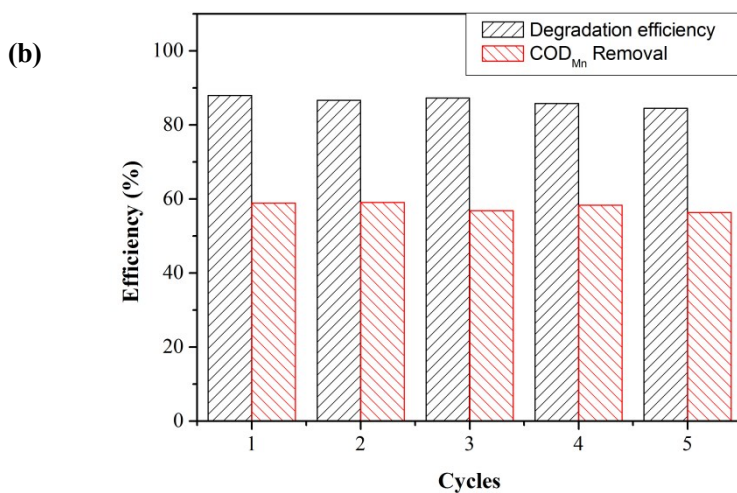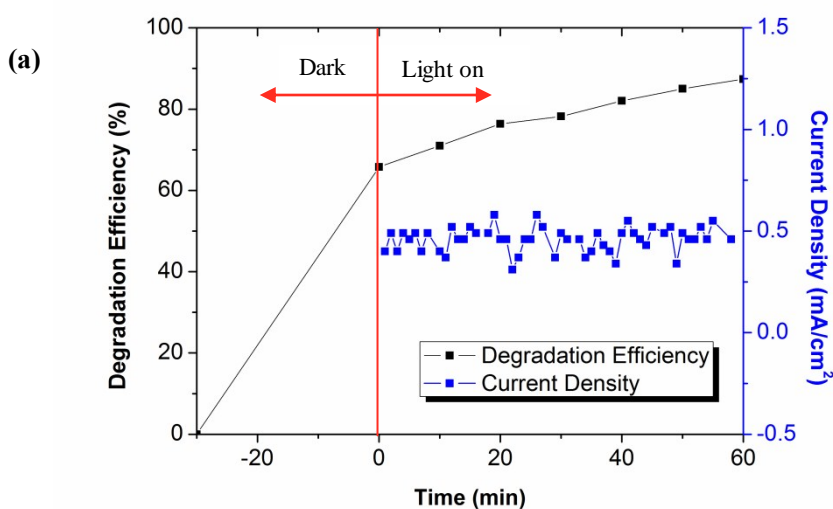
Figure 4. (a) degradation efficiency of RhB and the current density of the PFC with an external resistance of 1Ω (C_0=10mg/L, pH=7, $C_{(Na2SO4)}$=0.1mol/L); (b) cycled degradation efficiency of RhB and the COD_{Mn} removal rate; (c) current density in the cycles experiment.

3.3.3 Electrical energy efficiency

EEO (energy efficiency per order) is usually used to evaluate the treatment costs, which is defined as the electrical energy (kW·h) required to reduce the concentration of a pollutant by 1 order of magnitude, in a unit volume of contaminated water.[32] As the only energy input was two 2W LED lights, the EEO calculated for this photoelectrocatalysis system is 38.6 kW·h/m³,assuming the full use of all LED light energy by the PFC. Even so, the EEO of our established PFC system was quite low compared with other advanced oxidation processes, which is only 1/27 of a reported value (1075.3 kW·h/m³) for photodegradation of diazinon with UV/ZnO (14nm).[33] The power density of the external resistance (1Ω) was 0.54W/m³.

3.3.4 The function of cathodic Ag/AgCl/GO in two-chambered PFC with Fe anode

In the single-chambered PFC, anodic Ag/AgCl/GO functioned well in degradation and electricity generation. We found it can also function well as cathodic catalyst in a two-chambered PFC with Fe as anode. In the two-chambered reactor, the iron plate anode, supplied electrons for cathodic Ag/AgCl/GO. The cell voltage of the double-chambered PFC was 0.946V and potential of Ag/AgCl/GO cathode was 0.175V. Compared with the single-chambered PFC with Ag/AgCl/GO and $ZnIn_2S_4$, the degraded RhB in one hour increased by

12

129%, although the degradation efficiency was 54.23% (Fig. 5).

ESR spectrum was obtained from a mixture of RhB (10mg/L), Na_2SO_4 (0.1M) and spin trap DMPO (20 mM) in the anode chamber of PFC with anodic Ag/AgCl/GO and cathodic $ZnIn_2S_4$ catalysts (Fig. S3(a)). It indicated the actual generation of ·OH in the process. When Ag/AgCl/GO functioned as anodic catalyst, ·OH was formed from reaction of holes with OH^- or H_2O and the pollutants were oxidized mainly by ·OH. In the cathode chamber of PFC （Fe anode and Ag/AgCl/GO cathode), both DMPO/O_2·$^-$ and DMPO/·OH signal were detectable. That`s because the electrons mainly react with O_2 and generate O_2·$^-$, when Ag/AgCl/GO functions as cathodic catalyst. But O_2·$^-$is sensitive to the presence of proton and it may transform to form H_2O_2 or ·OH through series reactions.[34] So in the cathode chamber, oxidation of pollutants is mainly by ROS generated from reductive reaction of electron with oxygen.
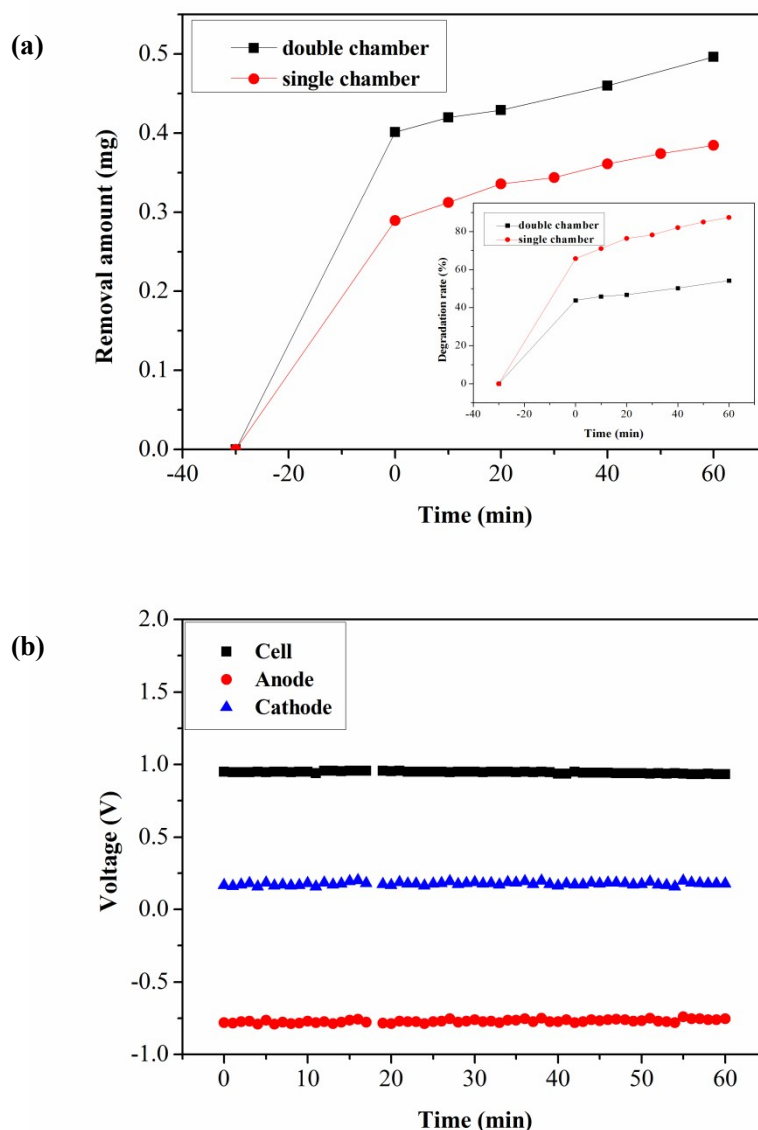
Figure 5. Degradation efficiency of RhB and the voltage in the two-chambered PFC with Fe-anode and Ag/AgCl/GO-cathode. "Single chamber" refers to the single-chambered PFC with Ag/AgCl/GO and ZnIn2S4 photo electrodes. "Double chamber" refers to the two-chambered PFC with Fe-anode and Ag/AgCl/GO-cathode

3.3.5 Other possible Configuration of PFC

With anodic Ag/AgCl/GO and cathodic $ZnIn_2S_4$, in two-chambered PFC system (Fig. S2), the rate constants over anode was 0.008 min^{-1} and cathode was 0.007 min^{-1}. In one chambered PFC system, the apparent rate constant (k) was 0.016 min^{-1}, higher than the sum (0.015 min^{-1}) in the two chamber system. PFCs with paired catalysts, Ag/AgCl/GO versus TiO_2

and/or TiO_2 versus $ZnIn_2S_4$ were also tested in the one chamber system (Fig. S1). Because the

CB and VB of TiO_2 (-0.1 VS.NHE for E_{CB}, +3.1 VS.NHE for E_{VB}) were almost the same

with Ag/AgCl/GO, the cell voltage of Ag/AgCl/GO versus TiO_2 was nearly zero in PFC. The

PFC performance of TiO_2 versus $ZnIn_2S_4$ was comparable to the PFC with Ag/AgCl/GO and

$ZnIn_2S_4$. TiO_2-electrode can only be excited by UV light. So the one chamber Ag/AgCl/GO-

$ZnIn_2S_4$ PFC system we constructed was efficient, convenient and more applicable under vis-

ible range.

3.4 Effect of the parameters on the performance of PFC
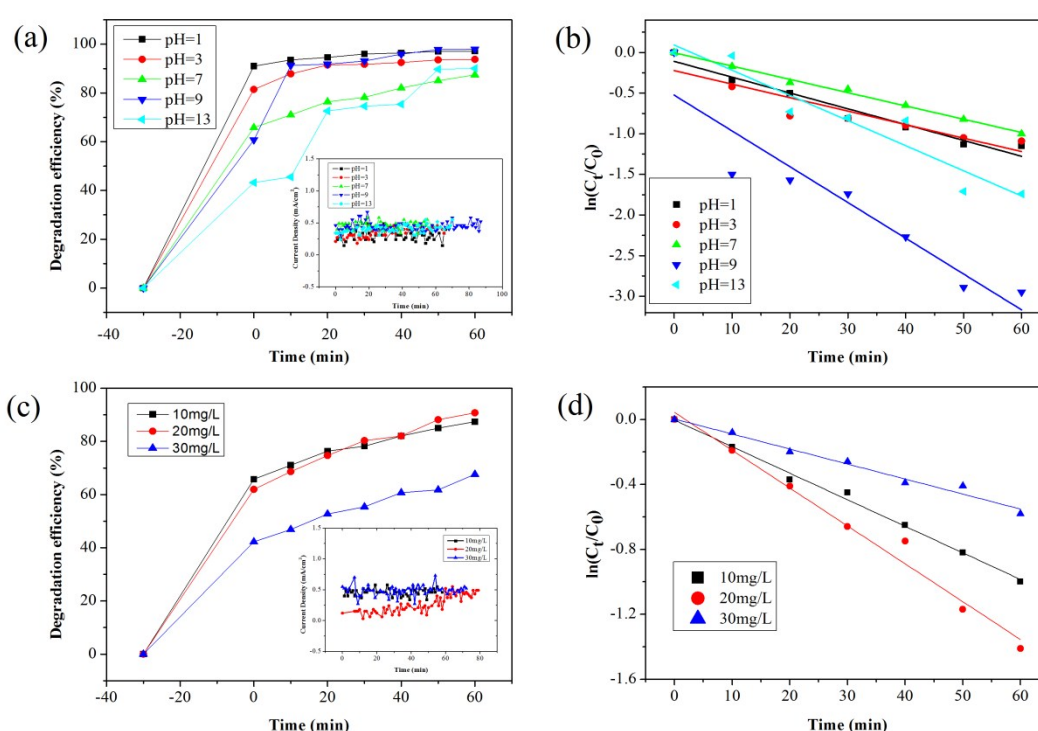

Figure 6. (a) The Degradation effiency of the PFC with different pH; insert: the current density of

the PFC with different pH; (b) The kinetic analysis of RhB degradation in the PFC with different

pH; (c) The Degradation effiency of the PFC with different initial concentration of RhB; insert:

the current density of the PFC with different initial concentration of RhB; (d) The kinetic analysis

of RhB degradation in the PFC with different initial concentration of RhB.

3.4.1 Effect of pH

Since the wide pH ranges in industrial effluents, it is important to study the effects of pH

on the degradation of RhB. As already described, 87.4% degradation of RhB was obtained in

our PFC with Ag/AgCl/GO-based photoanode and ZnIn$_2$S$_4$-based photocathode under a neutral pH in 60 minutes (Fig. 6a). Under alkaline conditions, 98% and 90% was reached at a pH value of 9 and 13 respectively. The enhancement was due to the presence of OH$^-$ which helps efficient holes scavenging and production of hydroxyl radicals. But when pH was too high, the oxygen evolution may occurred because of •OH radicals ((Eqs. (1)).[35] The produced oxygen on the surface of electrode inhibits adsorption of RhB to the electrode. Thus the degradation of RhB was influenced.

$$2 \cdot OH \rightarrow 2H^+ + O_2 + 2e^- \tag{1}$$

However in acidic conditions, degradation efficiency was 97.1% at pH 1 and 93.8% at pH 3. This might be explained by that the acid condition inhibited the oxygen evolution. So the adsorption of RhB would be enhanced. Although the decreasing of pH affected generation of •OH to some extent, the generated hydroxyl radical was enough for the degradation of low concentration of RhB. After 30 minutes darkness, the adsorption quantity of RhB increased with increase in pH value. The kinetic analysis shows that the degradation of RhB follows the pseudo-first order (Fig. 6b). The apparent rate constant (k) for pH 1, 3, 7, 9 and 13 was 0.019, 0.016, 0.016, 0.044 and 0.03 min^{-1} respectively. The photogenerated current in the PFC was the highest (about 0.5mA/cm^2) in neutral or basic/alkaline conditions (pH=7 or 9). When the pH of the solution was too high or too low, the electricity production decreased.

3.4.2 Effect of initial concentration of RhB

Fig. 6(c, d) shows the effect of the initial concentration of RhB on the performance of PFC in terms of the degradation efficiency of RhB, and values of degradation rate constant which corresponds to the slope of the kinetics curves (ln(C$_t$/C$_0$-t)). When the initial concentration of RhB increased from 10mg/L to 20mg/L, the degradation efficiency was comparable, even higher. It was because the anodic oxidation rate was higher than the RhB adsorption rate to the anode. The hydroxyl radical generated was enough to degrade all RhB diffused to the anode. But with the continued increase of concentration, the RhB adsorption rate was higher. Only part of RhB on the anode could be degraded timely. It dropped to 67.6% when the concentration increased to 30 mg/L. The changes of apparent rate constant with different concentration of RhB had a similar tendency with the degradation efficiency. The apparent

16

rate constant for 20mg/L was 0.023min^{-1} which was higher than 0.016 min^{-1} for 10mg/L and 0.009 min^{-1} for 30mg/L. The value of current density with 10mg/L RhB initial concentration was comparable with 30mg/L, but it decreased to 0.2mA/cm^2 when the concentration was 20mg/L. The electricity production could be influenced by many factors, such as the concentration of substrate, electrode reaction, adsorption activity on surface of electrodes, ions in electrolyte and so on. In theory, the more sufficient the substrate is, the higher electricity generated. But in our one chamber system, different concentration of substrate may lead to other reactions, so when the RhB concentration increased from 10mg/L to 20mg/L, the generated electricity was decreased.

Conclusions

In summary, stainless steel based PFC with anodic Ag/AgCl/GO and cathodic $ZnIn_2S_4$ illuminated by 2W LED, efficiently removed RhB (87.4%) with 1Ω external resistance (versus the 67.8% removal under OCV). The higher degradation activity of Ag/AgCl/GO electrode defines its anodic function for supplying relatively richer electrons than $ZnIn_2S_4$ electrode. Degradation mechanism in the PFC was discussed from ESR studies. The anodic degradation over Ag/AgCl/GO mainly occurs by oxidative holes, while the cathodic degradation over $ZnIn_2S_4$ is because of reduction of oxygen over conductive band and formation of oxidative radicals. When the Fe anode supplied electrons, Ag/AgCl/GO functions as cathodic catalyst and degrades pollutants mainly by $O_2\cdot^-$. The effect of pH, initial RhB concentration on cell voltage and degradation rate was studied. The single-chambered PFC can operate in a broad range of pH, low acidic pH or high alkaline pH can promote degradation. It is efficient, convenient and more applicable under illumination in visible range.

Acknowledgment

References

1.   N. Abdullah and S. K. Kamarudin, *Journal of Power Sources*, 2015, **278**, 109-118.

2.   Y. Liu, J. Li, B. Zhou, H. Chen, Z. Wang and W. Cai, *Chemical communications*, 2011, **47**, 10314-10316.

3.   K. Li, H. Zhang, T. Tang, Y. Xu, D. Ying, Y. Wang and J. Jia, *Water research*, 2014, **62**, 1-10.

4.   Y. Liu, J. Li, B. Zhou, X. Li, H. Chen, Q. Chen, Z. Wang, L. Li, J. Wang and W. Cai, *Water research*, 2011, **45**, 3991-3998.

5.   Q. Chen, J. Li, X. Li, K. Huang, B. Zhou, W. Cai and W. Shangguan, *Environmental science & technology*, 2012, **46**, 11451-11458.

6.   J. Li, J. Li, Q. Chen, J. Bai and B. Zhou, *Journal of hazardous materials*, 2013, **262**, 304-310.

7.   Y. Xu and M. A. Schoonen, *American Mineralogist*, 2000, **85**, 543-556.

8.   H. Zhang, J. Xuan, H. Xu, M. K. H. Leung, H. Wang, D. Y. C. Leung, L. Zhang and X. Lu, *Energy Procedia*, 2014, **61**, 246-249.

9.   H. Zhang, X. Fan, X. Quan, S. Chen and H. Yu, *Environmental science & technology*, 2011, **45**, 5731-5736.

10.   M. Zhu, P. Chen and M. Liu, *ACS nano*, 2011, **5**, 4529-4536.

11.   M. Zhu, P. Chen and M. Liu, *Langmuir : the ACS journal of surfaces and colloids*, 2013, **29**, 9259-9268.

12.   W. Li, Z. Ma, G. Bai, J. Hu, X. Guo, B. Dai and X. Jia, *Applied Catalysis B: Environmental*, 2015, **174-175**, 43-48.

13.   X. Yao, X. Liu, D. Zhu, C. Zhao and L. Lu, *Catalysis Communications*, 2015, **59**, 151-155.

14.   J. Hou, C. Yang, Z. Wang, Q. Ji, Y. Li, G. Huang, S. Jiao and H. Zhu, *Applied Catalysis B: Environmental*, 2013, **142-143**, 579-589.

15.   N. Zhang, Y. Zhang and Y. J. Xu, Nanoscale, 2012, 4, 5792-5813.

16.   N. Zhang, M. Q. Yang, S. Liu, Y. Sun and Y. J. Xu, Chemical reviews, 2015, 115, 10307-10377.

17.   N. Zhang and Y.-J. Xu, CrystEngComm, 2016, 18, 24-37.

18.   B. Gao, L. Liu, J. Liu and F. Yang, Applied Catalysis B: Environmental, 2014, 147, 929-
        939.

19.   Z. Lei, W. You, M. Liu, G. Zhou, T. Takata, M. Hara, K. Domen and C. Li, *Chemical
        communications*, 2003, DOI: 10.1039/b306813g, 2142.

20.   K.-W. Cheng and C.-J. Liang, *Solar Energy Materials and Solar Cells*, 2010, **94**, 1137-
        1145.

21.   W. S. Hummers Jr and R. E. Offeman, *Journal of the American Chemical Society*, 1958,
        80, 1339-1339.

22.   B. Gao, L. Liu, J. Liu and F. Yang, *Applied Catalysis B: Environmental*, 2013, **129**, 89-97.

23.   J. Zhao, T. Wu, K. Wu, K. Oikawa, H. Hidaka and N. Serpone, *Environmental science &
        technology*, 1998, **32**, 2394-2400.

24.   J. Yang, W. Liao, Y. Liu, M. Murugananthan and Y. Zhang, *Electrochimica Acta*, 2014,
        144, 7-15.

25.   S. Rasalingam, R. Peng and R. T. Koodali, *Applied Catalysis B: Environmental*, 2015,
        174-175, 49-59.

26.   X. Yu, Y. Zhang and X. Cheng, *Electrochimica Acta*, 2014, **137**, 668-675.

27.   Y. Hou, X. Li, Q. Zhao, X. Quan and G. Chen, *Environmental science & technology*,
        2010, **44**, 5098-5103.

28.   X. Zhao and Y. Zhu, *Environmental science & technology*, 2006, **40**, 3367-3372.

29.   H. Liu, S. Cheng, M. Wu, H. Wu, J. Zhang, W. Li and C. Cao, *The Journal of Physical
        Chemistry A*, 2000, **104**, 7016-7020.

30.   Y. Fu, P. Xiong, H. Chen, X. Sun and X. Wang, *Industrial & Engineering Chemistry Re-
        search*, 2012, **51**, 725-731.

31.   S. Chai, G. Zhao, Y. N. Zhang, Y. Wang, F. Nong, M. Li and D. Li, *Environmental science
        & technology*, 2012, **46**, 10182-10190.

32.   N. Daneshvar, A. Aleboyeh and A. R. Khatae, *Chemosphere*, 2005, **59**, 761-767.

33.   N. Daneshvar, S. Aber, M. Seyeddorraji, A. Khatae and M. Rasoulifard, *Separation and
        Purification Technology*, 2007, **58**, 91-98.

34.   S. Song, J. Fan, Z. He, L. Zhan, Z. Liu, J. Chen and X. Xu, *Electrochimica Acta*, 2010, **55**, 3606-3613.

35.   W. Luo, J. G. Muller and C. J. Burrows, *Organic letters*, 2001, **3**, 2801-2804.
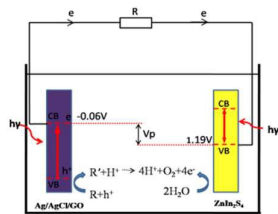
A PFC with anodic Ag/AgCl/GO and cathodic $ZnIn_2S_4$ catalysts was constructed for organic

compounds degradation and electricity generation.